Discharge Characteristics of Long SF_6 Gas Gap with and Without Insulator in GIS Under VFTO and LI

Tao Wen, Qiaogen Zhang, Jingtan Ma, Can Guo, Haoyang You, Yifan Qin, Yu Yin, Weidong Shi and Weijiang Chen, *Member, CSEE*

***Abstract*—Gas insulator switchgears (GISs), widely used in electric power systems for decades, have many advantages due to their compactness, minimal environmental impact, and long maintenance cycles. However, very fast transient overvoltage (VFTO) increases caused by a rise in voltage levels can lead to GIS insulation failures. In this paper, a generating system of VFTO and standard lightning impulse (LI) is established. The insulation characteristics of SF_6 gas with and without insulators under VFTO and standard LI are investigated. Experimental results show that the 50% breakdown voltages of the inhomogeneous electric field rod-plane gap under positive VFTO and standard LI are higher than that under negative VFTO and standard LI. The research shows that the 50% breakdown voltage under VFTO could be lower than that under standard LI at 0.5 MPa for the negative polarity. Moreover, the polarity effect of the insulator without defect is different from that with defect. Similarly, the breakdown voltage of the defective insulator under VFTO could be lower than that under standard LI by 8%. The flashover channel under VFTO is seen as more than that under standard LI. Based on the analysis of discharge images and experimental results, it is concluded that the polarity effect is related to the distortion effect of ion clusters formed by SF_6 on the electric field. Additionally, the steepness and front time of impulse plays an important role in the initiation and further development of discharge on insulator surface. Finally, the research shows that different discharge characteristics between VFTO and standard LI may be caused by different wave fronts and oscillation on the tails of the impulses.**

***Index Terms*—Breakdown voltage, discharge characteristic, gas insulated switchgear (GIS), lightning impulse (LI), space charge, very fast transient overvoltage (VFTO)**

I. INTRODUCTION

Manuscript received April 30, 2015; revised August 2, 2015; accepted August 27, 2015. Date of publication September 30, 2015; date of current version September 16, 2015. This work was supported by National Basic Research Program of China (973 Program) and Science and Technology Project of SGCC "Research on the Application of VFTO Key Techniques in Ultra High GIS Substation" (GYB17201400111).

T. Wen, Q. G. Zhang, J. T. Ma, C. Guo, H. Y. You, and Y. F. Qin are with the State Key Laboratory of Electrical Insulation and Power Equipment, Xi'an Jiaotong University, Xi'an 710049, China (e-mail: hv.wentao@stu.xjtu.edu.cn).

Y. Yin and W. D. Shi are with the China Electric Power Research Institute, Beijing 100192, China (e-mail: wdshi@epri.sgcc.com.cn).

W. J. Chen is with the State Grid Corporation of China, Beijing 100031, China (e-mail: chenwj@whvri.com).

Digital Object Identifier 10.17775/CSEEJPES.2015.00030

GAS insulator switchgears (GISs) are widely used in electric power systems for their many advantages in compactness, minimal environmental impact, and long maintenance cycles [1]. However, the disconnector operation in GIS can generate very fast transient overvoltage (VFTO), which varies from 1 MHz to 100 MHz [2], with maximum amplitude reaching 2.5 p.u. [3]. The VFTO can harm the insulation of the GIS, especially when voltage levels reach 330 kV or higher [4]. Data show that at high voltage levels, there are more insulation failures of GIS caused by VFTO than caused by lightning impulse (LI), thus drawing the attention of researchers in the field of high voltage.

SF_6 gas insulation characteristics [5]–[7] have been studied extensively and a large number of research results are available in the literature. S. Okabe *et al*. [11] have experimentally proven that for a SF_6 quasi-uniform electric field gap, the minimum breakdown voltage of positive polarity is higher than that of negative polarity under VFTO and standard LI. However, in an SF_6 highly inhomogenous electric field, the polarity effect was reversed and the minimum breakdown voltage of VFTO could be lower than that of standard LI [8], [9]. For example, in the non-uniform electrode gap with gap distance $d = 30$ mm and field utilization factor $\eta = 0.036$, the minimum breakdown voltage under VFTO (157.0 kV) (oscillation frequency $f = 2.7$ MHz, damping time constant $\tau = 25.6$ μs) is lower than that under standard LI (198.6 kV) with SF_6 up to absolute pressures 0.5 MPa. Moreover, when the local field enhancement appeared on the insulator surface, the breakdown voltage under VFTO could be lower than that under standard LI by 10%–20% [10].

However, other results have indicated that the breakdown voltage of insulator under VFTO was not lower than that under standard LI even though the non-uniform field was appeared [11]. Also, the gas gaps and insulators used in the studies were simplified models in small sizes (no more than 30 mm), which were inappropriate for simulation of the real situation. Therefore, the theoretical study of discharge characteristics and mechanisms of long SF_6 gaps with and without insulator is a valid research direction.

In this paper, a study of the discharge characteristics of SF_6 gas with and without insulator under VFTO and standard LI up to several megavolts is described. A mechanism of space charge model is proposed to illustrate the different discharge characteristics between VFTO and standard LI in SF_6.

II. Experimental Setup and Method

A schematic of the experimental set-up used in this work is shown in Fig. 1. It consists of an oil-immersed Marx generator and simulation GIS bus, generating standard LI with non-oscillating and VFTO with single frequency oscillating up to 8.1 MHz (see Fig. 2). Front time of the first wave T_{f}, wave tail time T_{t}, oscillation frequency f, and oscillating coefficient ξ are the four major parameters of VFTO. Oscillating coefficient is proposed to clarify the wave oscillation amplitude. ξ here is defined as:

$$\xi = \frac{(V_1 - V_2)/2}{V_1 - (V_1 - V_2)/2} \tag{1}$$

where, V_1 and V_2 are the first peak value and the first trough value of the VFTO, respectively. V_{s} is used as a reference to define the wave tail time of the VFTO.

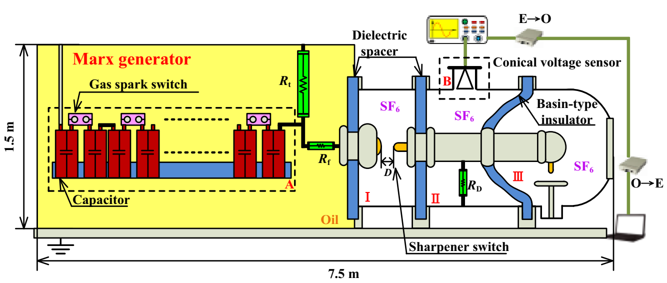

Fig. 1. Schematic diagram of VFTO generating system.

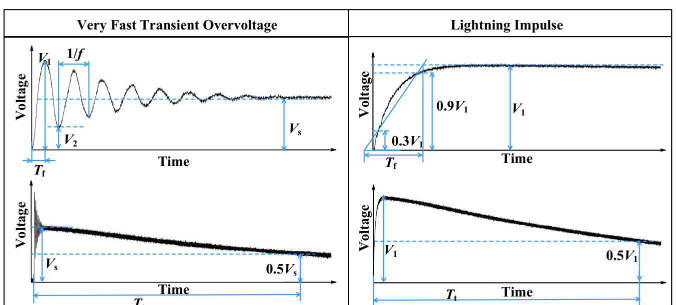

Waveform Parameters				Waveform Parameters	
T_f	T_t	f	ξ	T_f	T_t
49 ns	46.57 µs	8.1 MHz	0.35~0.80	1.12 µs	45.63 µs

Fig. 2. Typical voltage waveforms of VFTO and LI.

A newly developed conical voltage sensor is used for the measurement of standard LI and VFTO, as shown in Fig. 3. The fast front time calibrating result and long wave tail calibrating result indicate that the response of the newly developed conical voltage senor is less than 7 ns, and it could also satisfy the measuring requirement of the impulse with wave tail around 50 μs accurately, as shown in Fig. 4. An oscilloscope (Tektronix DPO4104) of 1GHz in bandwidth and 5 Gs/s in sample rate is used to record the waveforms. The V-t curve of breakdowns is obtained by applying impulse voltages with different prospective peak values, and the 50% breakdown voltage derived by using the up-and-down method, according to IEC 60060-1 [12].

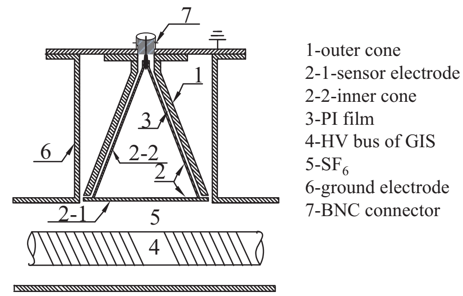

Fig. 3. Structure of the conical voltage sensor.

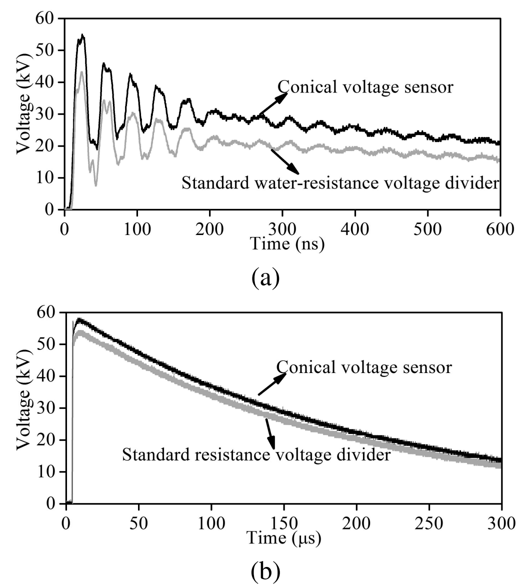

Fig. 4. Calibrating results of conical voltage sensor. (a) Fast front time calibrating result. (b) Long wave tail calibrating result.

The rod-plane electrodes and metal-contaminated insulator, shown in Fig. 5(a) and 5(b), is used to simulate local-field enhancement in GIS. The high voltage electrode in Fig. 5(a) is an 8-mm-radius hemispherically capped copper rod. A Rogowski copper electrode of 300 mm in diameter is used as the grounded plane. The electrode gap d is 112 mm in the test. The field nonuniformity factor f calculated by [13] was 10.58. The insulator used in this research is a 550 kV basin-type insulator. The high voltage electrode is a cylinder with the diameter from 130 mm to 150 mm. The inner diameter of the grounded cylinder is 555 mm. Steel needles with different length were attached to the insulator surface. The diameter of the needle is 0.5 mm, and its point tip radius is 0.1 mm. Both ends of the needle are not covered with adhesive, and the position of the needle on the insulator is adjustable. The test setups were installed in the chamber where the absolute pressures of SF_6 can vary from 0.1 MPa to 0.5 MPa. The ξ of VFTO stressed on the rod-plane electrodes and insulator was 0.35.

III. Experimental Results and Discussions

A. Discharge Characteristics of SF_6 Gas Without Insulator

In the literature, the breakdown voltage for a non-uniform field (typically the rod-plane gap) is reported to be lower when

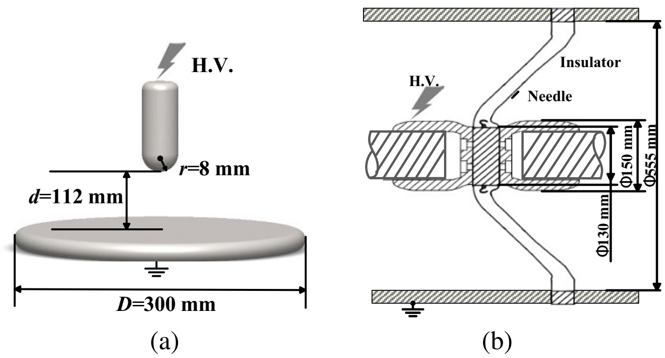

Fig. 5. Test setups. (a) Rod-plane electrode. (b) Metal-contaminated insulator.

the rod electrode is stressed by positive polarity voltages [14], [15]; the polarity effect for the rod-plane gap in this study, however, has been found to be different, as shown in Fig. 6, which shows the relationship between the breakdown voltage of the SF_6 gap and the gas pressure under different voltage polarities. In positive polarity, the 50% breakdown voltage is higher than that in negative polarity for both VFTO and standard LI. Interestingly, at 0.5 MPa the 50% breakdown voltage under VFTO is lower than that under standard LI for the negative polarity. In other words, VFTO with negative polarity is a bigger threat to the insulation of GIS than standard LI.

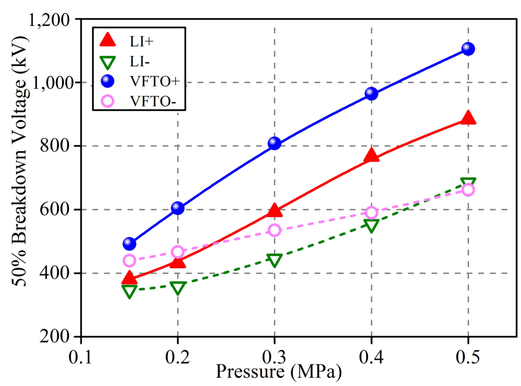

Fig. 6. 50% Breakdown voltage vs. gas pressure for 112 mm rod-plane gap under VFTO and standard LI.

Fig. 7 shows the V-t curves of the rod-plane gap under VFTO and LI at different pressures. It can be seen from Fig. 7(a) that the V-t curves of VFTO and standard LI intersect for positive or negative polarity at a lower pressure. Similarly, at higher pressure the V-t curve of VFTO for negative polarity falls below that of standard LI, as shown in Fig. 7(b).

B. Discharge Characteristics of SF_6 Gas with Insulator

The breakdown voltage of insulator with and without defect of a 15-mm needle is shown in Fig. 8 and the corresponding discharge images are shown in Fig. 9. The length x is defined as the distance between the inner electrode and the needle.

The breakdown voltage of insulator with and without defect under VFTO or standard LI in negative polarity is higher than that in positive polarity, which is opposite to the polarity effect

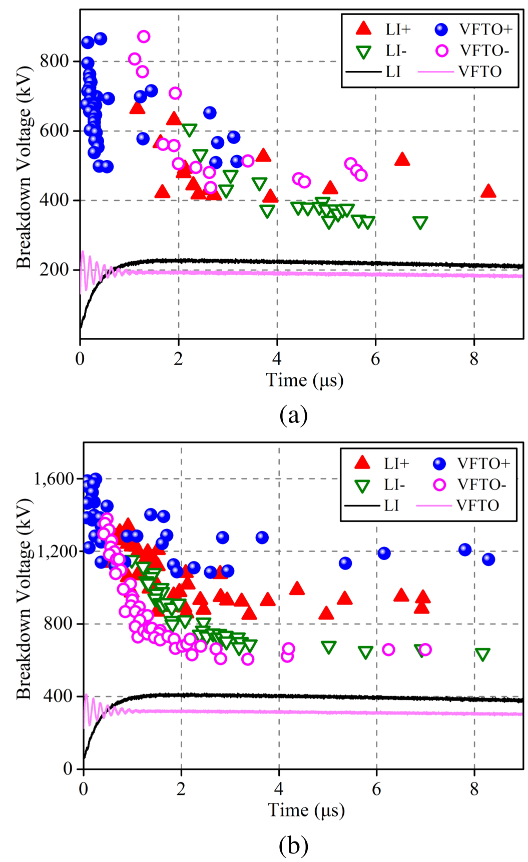

Fig. 7. Voltage-time curves of 112 mm rod-plane gap under VFTO and standard LI. (a) $P = 0.2$ MPa. (b) $P = 0.5$ MPa.

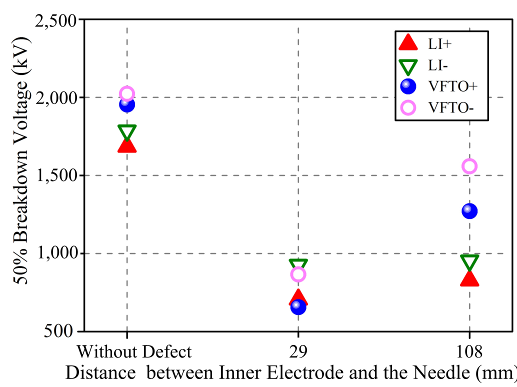

Fig. 8. Breakdown voltage of insulaor with and without defect ($P = 0.5$ MPa).

of SF_6 gas gap with quasi-uniform field. When the insulator is contaminated by a needle, the breakdown process contains two steps, i.e., the breakdown between inner electrode and the needle as well as the breakdown between the needle and outer electrode [16]. In Fig. 9(b), a partial arc bridges the inner electrode and needle initially. The electric field in front of needle is non-uniform, resulting in the breakdown voltage for VFTO or LI in positive polarity being lower than that in negative polarity.

In this study, the charge was generated with relatively high density on the insulator surface near the needle under VFTO and standard LI [17]. These surface charges interact with the

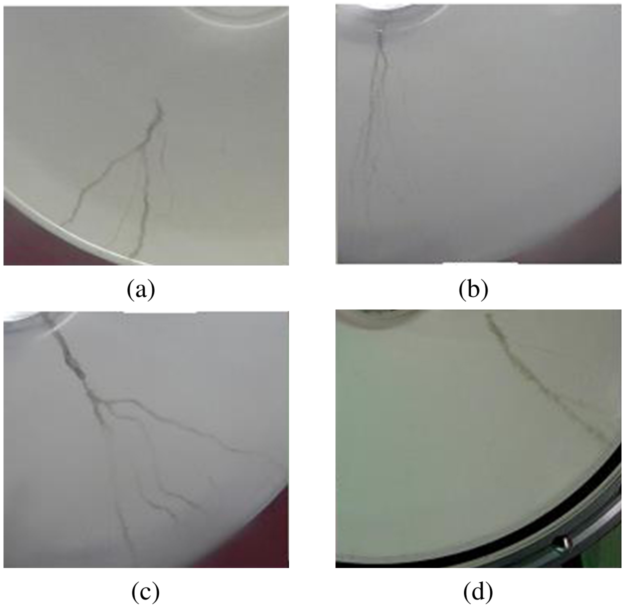

Fig. 9. Discharge images of insulator with and without defect. (a) Insulator without defect under VFTO. (b) Insulator with defect under VFTO (x = 29 mm). (c) Insulator with defect under VFTO (x = 108 mm). (d) Insulator without defect under standard LI.

charges of streamer head in developing a breakdown channel shown in Fig. 10. Thus, two forces act on the streamer head, i.e., $\boldsymbol{F}_{\mathbf{t}}$ formed by the external field and $\boldsymbol{F}_{\mathbf{n}}$ from the surface charges [16]. When the positive impulse is applied on the inner electrode, shown in Fig. 10(a), the positive charges accumulate on the insulator surface near the needle [17]. Thus, the streamer head near the inner electrode is attracted to the insulator surface. The interaction of the partial arc and insulator will cause damage to the insulator, leaving a dark trace on the insulator surface [18]. The streamer head near the outer electrode is instead pushed away from the insulator surface where insulator damage is less probable. Only the light trace is observed, which are proven by discharge traces shown in Fig. 9(b) and Fig. 9(c). The case that inner electrode biased negatively is shown in Fig. 10(b). The charges could hardly accumulate on the insulator surface without defect [17] and only $\boldsymbol{F}_{\mathbf{t}}$ acts on the streamer head. Moreover, the field of insulator surface is more uniform because of the shielding effect of the inner protruding electrode. So, the discharge hardly develops on the insulator surface near the inner electrode shown in Fig. 9(a).

In order to obtain the distribution of surface electric field of the insulator and further understand the accumulation of the surface charges, Ansoft was used to simulate the total surface electric field $\boldsymbol{E}$, its normal component $\boldsymbol{E}_{\mathbf{n}}$ and tangential component $\boldsymbol{E}_{\tau}$ of the insulator with and without defect, as shown in Fig. 11. When computing, 1000 kV static voltage was stressed on the high voltage electrode.

As shown in Fig. 11(a), the distribution of surface electric field of the insulator without defect is approximately uniform. The maximal $\boldsymbol{E}$ and $\boldsymbol{E}_{\mathbf{n}}$ both appear on the concave side of the insulator close to the inner conductor. When the insulator is contaminated by the needle, the surface electric field increases

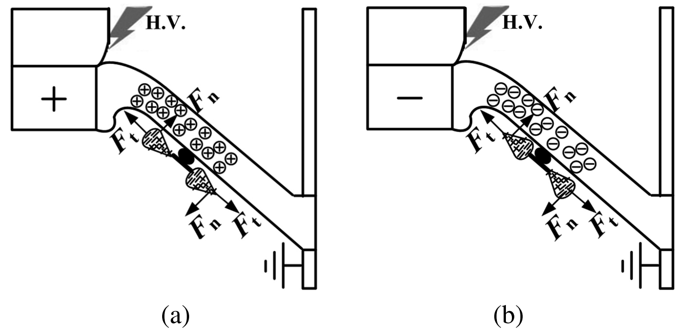

Fig. 10. Schematic discharge diagram of insulator with defect. (a) Positive polarity. (b) Negative polarity..

significantly to a maximum of 6 times more than that of the insulator without defect.

Fig. 11(b) and Fig.11(c) indicate that $\boldsymbol{E}_{\mathbf{n}}$ near the needle is much stronger than $\boldsymbol{E}_{\tau}$. Large quantities of charges are accumulating in the insulator surface close to the needle, resulting where the breakdown voltage of insulator with defect decreases significantly when compared with that without defect. Apart from that, when comparing Fig. 10(b) with Fig. 10(c), the maximal $\boldsymbol{E}$ (x = 29 mm) and $\boldsymbol{E}_{\mathbf{n}}$ (x = 29 mm) are larger than the maximal $\boldsymbol{E}$ (x = 108 mm) and $\boldsymbol{E}_{\mathbf{n}}$ (x = 108 mm), which causes that the breakdown voltage of the needle near the high electrode is the lowest, as verified in Fig. 8.

To investigate the effect of the length of the needle contaminant l on the insulator under VFTO and standard LI, various lengths of needles were used keeping the defect location x at 108 mm. Fig. 12 shows the corresponding results of positive and negative VFTO and LI flashover tests indicating that the 50% breakdown voltage decreases with increasing needle length. For $l < 15$ mm, the 50% breakdown voltage under VFTO is higher than that with standard LI. However, VFTO decreases significantly for $l > 15$ mm, compared with standard LI.

C. Effect of Voltage Waveform

Waveform conversion factor K is proposed [14] to clarify the effect of voltage waveform on discharge characteristics, which is defined by the ratio of 50% breakdown voltage under VFTO to that under standard LI. The factor K of rod-plane gap and insulator are shown in Fig. 13 and Fig. 14. Fig. 13 shows that with increasing pressure, K decreases and when pressure reaches 0.5 MPa, K becomes less than 1, which can be explained by the restraining effect of space charge accumulation under oscillating impulse with increasing pressure, mentioned in Section III A.

Previous research shows that micro discharge in the gas near insulator surface such as streamer corona caused by fixed metal particles is the prerequisite condition for charge accumulation under impulse voltage [17]. For VFTO, a great quantity of charges is absorbed onto the surface of the defective insulator by streamer at the rising slope of oscillating impulse [2]. A strong reverse electric field is formed when the impulse decreases rapidly, resulting in the so-called

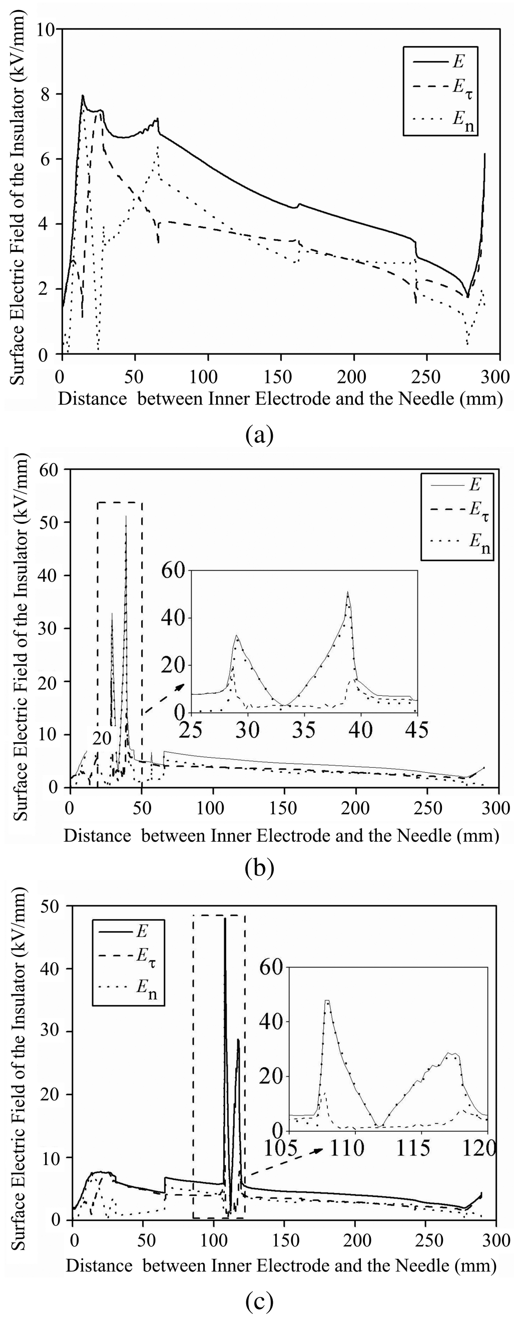

Fig. 11. $\boldsymbol{E}$, $\boldsymbol{E}_{\tau}$ and $\boldsymbol{E}_{\mathbf{n}}$ of insulator. (a) Without defect. (b) With defect, $x =$ 29 mm, 1000 kV. (c) With defect, $x = 108$ mm, 1000 kV.

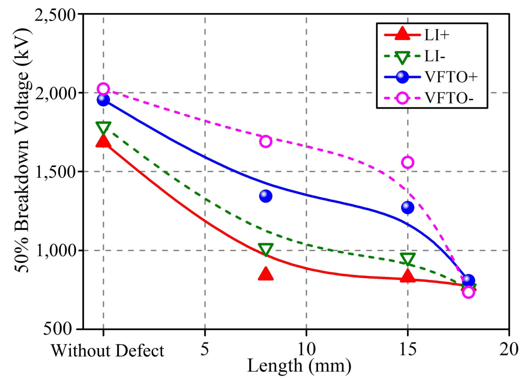

Fig. 12. Breakdown voltage vs. needle length for insulator with defect under VFTO and standard LI. ($P = 0.5$ MPa, $x = 108$ mm).

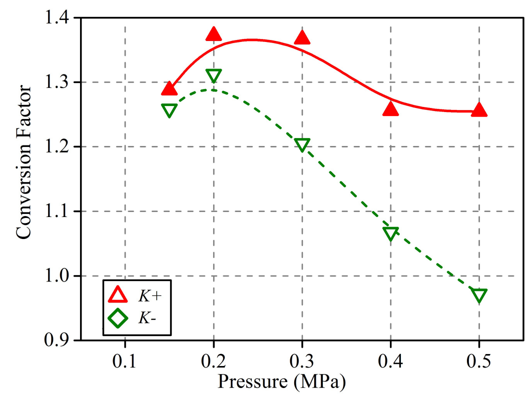

Fig. 13. Waveform conversion factor vs. gas pressure for 112 mm rod-plane gap.

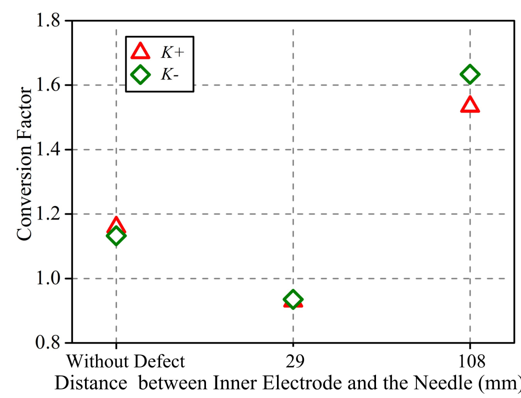

Fig. 14. Waveform conversion factor of insulator with and without defect.

"back discharge" [19], which occurs between the channel and surrounding deposited charges. Back discharge decreases the shielding effect of surface charges and also increases the conductivity of streamer channels so that the leader can be triggered easily. As a result, the breakdown voltage of the defective insulator under VFTO can be lower than that under standard LI by 8%, as shown in Fig. 14.

It is interesting to observe that multi-channels are formed on the insulator surface when VFTO is applied, as shown in Fig. 9(b) and Fig. 9(c), while the discharge channels on insulator surface under LI are fewer than those under VFTO, shown in Fig. 9(d). This phenomenon is caused by the inter-shielding effect of electron avalanches [20]. Since the delay time of primary electrons are different, some preceding avalanches develop ahead of time and form the space charge field, which changes the applied electric field. And this restrains the adjacent electron avalanche called posterior avalanche. With decreasing front time of pulse, the difference in formation of primary electrons decreases; the inter-shielding effect of electron avalanches also decreases, leading to an increase of discharge branches. Therefore, the phenomenon of decreased pulse front time increasing the discharge branch number can be clarified.

IV. Conclusion

The discharge characteristics and discharge development of SF_6 gas with and without insulator under VFTO and standard LI was studied. Experimental results indicated that the breakdown voltage for VFTO or standard LI in positive polarity is higher than that in negative polarity and the breakdown voltage of VFTO could be lower than that of standard LI at high gas pressure. The breakdown voltage of insulator under VFTO or standard LI in negative polarity is higher than that in positive polarity and the breakdown voltage of defective insulator under VFTO could be lower than that under LI by 8%. The different characteristics of discharge are caused by different conditions such as different applied voltages, polarities, insulating mediums, and gas pressures.

References

[1] W. Chen, X. Yan, S. Wang, C. Wang, Z. Li, M. Dai, C. Li, W. Liu, H. Chen, Q. Zhang, G. Wei, and M. Zhang, "Recent progress in investigation on very fast transient overvoltage in gas insulated switchgear," *ProcEedings of CSEE*, vol. 31, no. 31, pp. 1–11, Nov. 2011.

[2] Q. Zhang, J. Jia, L. Yang, F. Tao, and Y. Qiu, "Mechanism of discharge development in SF_6 with and without spacers under fast oscillating impulse condition," *Journal of Applied Physics*, vol. 98, pp. 103301(1)–103301(5), Nov. 2005.

[3] J. Meppelink, K. Diederich, K. Feser, and W. Pfaff, "Very fast transients in GIS," *IEEE Transactions on Power Delivery*, vol. 4, no. 1, pp. 223–233, Jan. 1989.

[4] Y. Yamagata, Y. Nakada, K. Nojima, M. Kosakada, J. Ozawa, and I. Ishigaki, "Very fast transients in 1000 kV gas insulated switchgear," in *IEEE Transmission and Distribution Conference*, 1999, pp. 501–508.

[5] W. Liu, L. Wang, W. Chen, M. Dai, Z. Li, and G. Yue, "Investigation of the VFTO related repeated breakdown processes in UHV GIS," *High Voltage Engineering*, vol. 37, no. 3, pp. 644–650, 2011.

[6] L. Zhang, Q. Zhang, S. Liu, Y. Yin, W. Shi, and W. Chen, "Insulation characteristics of UHV GIS under VFTO and lightning impulse," *High Voltage Engineering*, vol. 38, no. 2, pp. 335–341, 2012.

[7] B. Lee, Y. Baek, H. Choi, and S. Oh, "Impulse breakdown characteristics of the plane-to-plane electrode system with a needle-shaped protrusion in SF_6," *Current Applied Physics*, vol. 7, no. 3, pp. 289–295, 2007.

[8] S. Okabe, S. Yuasa, and S. Kaneko, "Evaluation of breakdown characteristics of gas insulated switchgears for non-standard lightning impulse waveforms-breakdown characteristics for non-standard lightning impulse waveforms associated with lightning surges," *IEEE Transactions on Dielectrics and Electric Insulation*, vol. 15, no. 2, pp. 407–415, 2008.

[9] G. Ueta, S. Kaneko, and S. Okabe, "Evaluation of breakdown characteristics of gas insulated switchgears for non-standard lightning impulse waveforms-breakdown characteristics under non-uniform electric field," *IEEE Transactions on Dielectrics and Electric Insulation*, vol. 15, no. 5, pp. 1430–1438, 2008.

[10] Q. Chen, Y. Wang, and X. Wei, "Spacer flashover in SF_6 under steep-fronted impulse voltages" in *Proceedings of 8th International Conference on Properties and Applications of Dielectric Materials*, Denpasar, Bali, Indonesia, 2006, 739–742.

[11] S. Okabe, M. Koto, F. Endo, and K. Kobayashi, "Insulation characteristics of GIS spacer for very fast transient overvoltage," *IEEE Transactions on Power Delivery*, vol. 11, no. 1, pp. 210–218, 1996.

[12] *IEC Standard for High-Voltage Test Techniques—Part 1: General Definitions and Test Requirements*, IEC 60060-1-2010, 2010.

[13] Y. Qiu, "Simple expression of field nonuniformity factor for hemispherically capped rod-plane gaps," *IEEE Transactions on Electric Insulator*, vol. EI-21, no. 4, pp. 673–675, Aug. 1986.

[14] G. Ueta, S. Kaneko, and S. Okabe, "Evaluation of breakdown characteristics of gas insulated switchgears for non-standard lightning impulse waveforms—Breakdown characteristics under non-uniform electric field," *IEEE Transactions on Dielectrics and Electric Insulation*, vol. 15, no. 5, pp. 1430–1438, 2008.

[15] F. Pinnekamp and L. Niemeyer, "Qualitative model of breakdown in SF_6 in inhomogeneous gaps," *Journal of Physics D: Applied Physics*, vol. 16, no. 7, pp. 1293–1302, 1983.

[16] B. Mazurek, J. Cross, and R. Heeswijk, "The effect of a metallic particle near a spacer on flashover phenomena in SF_6," *IEEE Transactions on Electric Insulator*, vol. 28, no. 2, pp. 219–229, 1993.

[17] F. Wang, Y. Qiu, W. Pfeiffer, and E. Kuffel, "Insulator surface charge accumulation under impulse voltage," *IEEE Transactions on DielectrIcs and Electric Insulation*, vol. 11, no. 5, pp. 847–854, 2004.

[18] M. Li and A. Vlastos, "Influence of impulse voltage waveshape on the flashover of clean and particle-contaminated spacers in SF_6 gas-insulated system," *IEEE Transactions on Power Delivery*, vol. 4, no. 1, pp. 326–334, 1989.

[19] O. Yamamoto, T. Hara, and T. Takuma, "The role of leader re-illumination in the development of surface discharges in SF_6 exposed to a very fast transient overvoltage," *Journal of Physics D: Applied Physics*, vol. 31, pp. 2997–3003, 1998.

[20] Q. Zhang, F. Tao, Z. Li, W. Ding, and A. Qiu, "Effect of pulse rise time on the glow discharge in nonuniform electric field," *IEEE Transactions on Plasma Science*, vol. 36, no. 4, pp. 1008–1009, 2008.

Tao Wen was born in Shaanxi Province, China, in 1990. He received the B.S. degree in electrical engineering from Xi'an Jiaotong University, Xi'an, China, in 2012. He is currently working toward a Ph.D. degree at the High Voltage Division, School of Electrical Engineering, and the State Key Laboratory of Electrical Insulation and Power Equipment.

Qiaogen Zhang received the B.S., M.S., and Ph.D. degrees in electrical engineering from Xi'an Jiaotong University, Xi'an, China, in 1988, 1991, and 1996, respectively. He is currently a Professor with the High Voltage Division, School of Electrical Engineering, and the State Key Laboratory of Electrical Insulation and Power Equipment, Xi'an Jiaotong University. His major research interests include outdoor insulation, pulse power technology, gas discharge, and its application.

Jingtan Ma was born in Henan, China in 1993. He received the B.S. degree from the Xi'an Jiaotong University, Shaanxi, China in 2014. He is currently working toward the M.S. degree in the High Voltage Division, School of Electrical Engineering, and the State Key Laboratory of Electrical Insulation and Power Equipment.

Can Guo was born in Shanxi, China, in 1990. He received the B.S. degree from the Xi'an Jiaotong University, Shaanxi, China in 2013. He is currently working toward the Ph.D. degree in the High Voltage Division, School of Electrical Engineering, and the State Key Laboratory of Electrical Insulation and Power Equipment.

Haoyang You was born in Hebei, China in 1993. He received the B. S. degree from the Xi'an Jiaotong University, Shaanxi, China in 2014. He is currently working toward the Master degree in the High Voltage Division, School of Electrical Engineering, and the State Key Laboratory of Electrical Insulation and Power Equipment.

Yifan Qin was born in Jiangsu, China, in 1992. He received the B.S. degree from the Xi'an Jiaotong University, Shaanxi, China in 2014. He is currently working toward the Master's degree in the High Voltage Division, School of Electrical Engineering, and the State Key Laboratory of Electrical Insulation and Power Equipment.

Yu Yin was born in Shaanxi Province, China, in 1975. He received the B.S. and Ph.D. degrees in electrical engineering from Tsinghua University, Beijing, China, in 1998 and 2004, respectively. He is currently a Senior Engineer with the High Voltage Department, China Electric Power Research Institute.

Weidong Shi was born in Guangdong Province, China, in 1966. He received the B.S. and M.S. degrees in electrical engineering from Xi'an Jiaotong University, Xi'an, China, in 1988 and 1991, respectively, and Ph.D. from Nagasaki University, Nagasaki, Japan, in 2001. He is currently a Senior Engineer with the High Voltage Department, China Electric Power Research Institute.

Weijiang Chen was born in Shandong Province, China, in 1958. He received the B.S. degree in electrical engineering from HeFei University of Technology, Hefei, China, in 1982. He received the M.S. degree in high voltage and insulation from China Electric Power Research Institute, Beijing, China, in 1985. He is currently a Professor with the Ultra High Voltage Department, State Grid Corporation of China.